



# Impact of process parameters and heat treatment on fused filament fabricated PLA and PLA-CF

Ribin Varghese Pazhamannil<sup>1</sup> · P. Govindan<sup>1</sup> · Abhilash Edacherian<sup>2</sup> · Haitham M. Hadidi<sup>3</sup>

Received: 30 August 2022 / Accepted: 8 October 2022 / Published online: 25 October 2022  
© The Author(s), under exclusive licence to Springer-Verlag France SAS, part of Springer Nature 2022

## Abstract

The fused filament fabrication 3D printing technique yields low mechanical strength components as a result of the layer-by-layer building process. The choice of appropriate pre-processing and post-processing procedures resulted in a significant improvement in the mechanical attributes. In this work, the effects of process parameters namely infill density, pattern, extruder temperature, layer thickness, and print speed on the ultimate tensile strength of polylactic acid and carbon fiber polylactic acid components were analyzed. For both the filaments, the maximum mechanical strength was found at 90% infill volume for the gyroid infill with a layer height of 0.1 mm at a print speed of 30 mm/s. The tensile properties were higher in carbon fiber reinforced tensile samples than in standard polylactic acid. The influence of thermal annealing on the mechanical strength of tensile samples (ASTM D638 Type IV) was also examined. Annealing polylactic acid samples at 95 °C for 60 min demonstrated a maximum tensile strength of 38.27 MPa, representing a 23.02% increase. Similarly, annealing reinforced thermoplastic samples at 95 °C for 120 min resulted in ultimate tensile strength of 42.49 MPa, representing a 14.01% increase. Heat treatment settings that are optimized can considerably improve the mechanical characteristics of the fused filament fabricated end-use products thereby enhancing the potential of the 3D printing sector.

**Keywords** Thermal annealing · Mechanical strength · Fused filament fabrication · Polylactic acid · Composite filament

## Abbreviations

3D	Three dimensional
ASTM	American Society for Testing and Materials
FFF	Fused filament fabrication
CNC	Computer numeric control
PLA	Polylactic acid
PLA-CF	Carbon fiber reinforced polylactic acid
CNC	Computer numeric control
CNF	Carbon nano fiber
XRD	X-ray diffraction

$T_g$	Glass transition temperature
PETG	Polyethylene terephthalate glycol
PETG-CF	Carbon fiber reinforced polyethylene terephthalate glycol
SEM	Scanning electron microscopy

## 1 Introduction

Additive manufacturing is a unique production process capable of fabricating customized objects without any structural limitations. The layer-by-layer paradigm rapidly gained popularity due to the non-wastage of materials unlike in the subtractive manufacturing process. 3D printing is mainly categorized into seven types based on the principle of formation of each layer of the target specimen [1–4]. The classification of 3D printing processes is described in Fig. 1. FFF is the largely used additive manufacturing process due to its simplicity, low cost, automated process, and no tooling advantages. FFF is based on thermoplastic-based material extrusion methodology. Application-specific filaments are

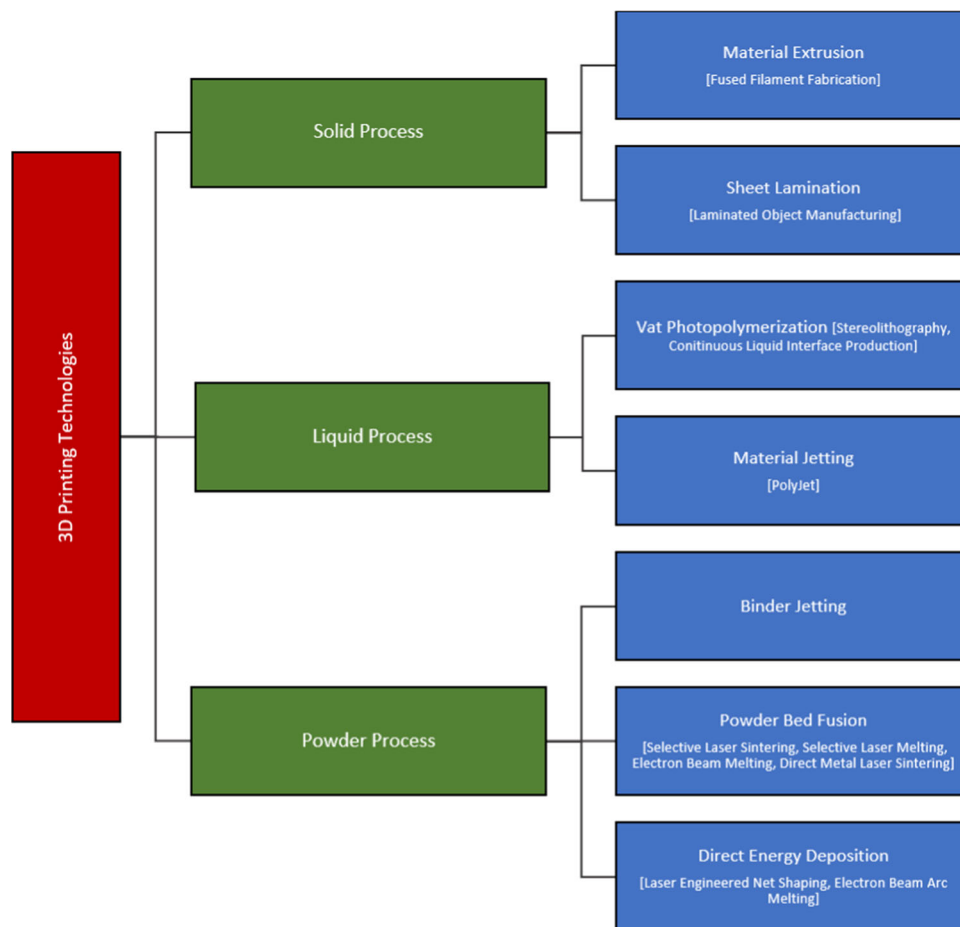
✉ Ribin Varghese Pazhamannil  
ribinvarghese18@gmail.com

<sup>1</sup> Department of Mechanical Engineering, Government College of Engineering Kannur, APJ Abdul Kalam Technological University, Kerala, India

<sup>2</sup> Department of Mechanical Engineering, College of Engineering, King Khalid University, Abha, Kingdom of Saudi Arabia

<sup>3</sup> Department of Mechanical Engineering, College of Engineering, Jazan University, Jazan, Kingdom of Saudi Arabia

Fig. 1 3D printing processes



available ranging from biodegradable PLA to strong metal and fiber-reinforced filaments [5–8]. This technology gained attention in many sectors such as medical, aerospace, architecture, fashion, consumer goods, education, electronics, etc. Artificial human organs, sockets, scaffold manufacturing for cells generation, patient-specific implants, drug transfer equipment, conductive components for sensing, electromagnetic interference protectors, rapid tooling, fire preventive filaments in aerospace, 4D printing, buildings and bridges, high strength to weight ratio automotive parts, microfluidic instruments, customized jewellery, etc. are a few recent applications of FFF [9–16].

Mechanical strength and surface quality of FFF are low when compared to injection molding, blow molding, etc. The anisotropic behavior of the end components is another limitation [17]. The stress-induced in the components due to the hot extrusion of a thermoplastic layer onto a previously formed cool layer affects its mechanical strength [18, 19]. The layer-upon-layer generation to form the final geometry causes stair-casing surface quality problems [20]. Proper pre-processing and post-processing techniques can overcome the above-mentioned drawbacks. Pre-processing

techniques include process parameter selection and adaptive slicing. Post-processing methods are categorized as mechanical, chemical, and thermal processes. Mechanical techniques include sand blasting, barrel finishing, sanding, CNC machining, etc. Vapor smoothing, dipping, electroplating, etc. fall under chemical processes [21–24]. Heat treatment methods for both surface and mechanical strength improvement had been studied in the past. Thermal annealing and normalizing processes [25] were found effective in the enhancement of mechanical properties. Process parameters and thermal annealing optimization are the selected methods for the analysis of its influence on ultimate tensile strength.

Zaldivar et al. [26] analyzed the influences of build direction on the tensile strength of ULTEM 9085 tensile specimens and obtained 46–85% strength of the injection molding process. The fibers in the loading direction improved the mechanical strength of dog bone samples. Perez et al. [27] analyzed the influence of various controllable factors on the surface characteristics of fused filament fabricated PLA samples. They demonstrated that the surface roughness reduced with a decrease in layer height and did not affect extruder temperature. The accuracy of parts and their dependence on the process variables were studied by Nath et al. [28].

Nozzle temperature of 375 °C produced the highest flexural strength for poly-ether-ether-ketone models. Reduction in layer height and higher infill percentage increased the mechanical strength. Hongbin Li et al. [29] showed that layer height is the most crucial variable influencing the tensile strength of the PLA samples. Therefore, the choice of optimum process parameters is required for attaining the highest possible mechanical properties.

Radoslaw et al. [30] showed that the flexural strength increases by 17% when PLA samples are annealed at 85 °C for 70 min. The degree of crystallinity also increased due to thermal annealing. Dong et al. [31] studied annealing effects on PLA composites and published that annealing of PLA-g-CNF at 70 °C doubles the storage modulus and the flexural modulus increase by approximately 152 times. Carbon fiber reinforced ASTM D638 Type-V PLA and normal PLA samples were tested for tensile strength and elastic modulus by Marcus Invy et al. [32]. Crystallinity increased by a maximum of 30% such that an increase in temperature resulted in higher crystallinity. Elastic modulus was higher for 15% reinforced PLA compared to that of normal PLA. Annealing at 85 °C for 2 h resulted in a slight enhancement of ultimate tensile strength. Sunil et al. [33] experimented with the influences of annealing on PETG, PETG-CF, PLA, and PLA-CF samples. PETG-CF showed a remarkable increase in tensile strength after annealing at 120 °C for 4–8 h. PLA increased its tensile strength by 17% and the ultimate tensile strength of PLA-CF became twice of unannealed samples. Rhugdhrivya et al. [34] demonstrated an increase of 89% for acrylonitrile butadiene styrene dog bone samples after annealing at 160 °C. Wootthikanokhan et al. [35] experimented with the influence of annealing at 100 °C for 60 min on three PLA composites having Cloisite30B, kenaf fiber, and h-BN as additives. Maximum heat deflection temperatures of 128 °C were obtained for kenaf fiber but decreased ultimate tensile strength. Cloisite30B and h-BN additives improved tensile strength slightly. Annealing effects on poly-ether-ether-ketone were studied by Anouar Magri et al. [36].

All of this research shows that the thermal annealing post-processing treatment influences the quality of components manufactured employing FFF, regardless of the filament material. The majority of the existing literature supports the improvement of mechanical characteristics during the heat treatment process. The objective of this study is to analyze the effects of process parameters on the mechanical strength of PLA and 20% PLA-CF filaments. The impact of annealing temperature and duration on the ultimate tensile strength is also studied, such that improved annealing conditions for mechanical property enrichment, if any, might be advantageous to the 3D printing sector. This work is innovative due to the extensive optimization analysis of the thermal annealing parameters on the strength enhancement of PLA and PLA-CF.

**Table 1** Selected process parameters of PLA

Process parameter	Levels		
Infill volume (%)	30	60	90
Infill pattern	Gyroid	Grid	Triangle
Print speed (mm/s)	30	45	60
Layer height (mm)	0.1	0.15	0.2
Nozzle temperature (°C)	200	210	220

**Table 2** Selected process parameters of PLA-CF

Process parameter	Levels		
Infill volume (%)	30	60	90
Infill pattern	Gyroid	Grid	Triangle
Print speed (mm/s)	30	45	60
Layer height (mm)	0.1	0.15	0.2
Nozzle temperature (°C)	210	220	230

## 2 Materials and methods

Raise3D Premium PLA and SUNLU PLA Carbon fiber were used as the thermoplastic filament for the FFF process. The filament diameter was 1.75 mm. PLA is a bio-degradable material and has many other advantages such as being simple to work, reliable, and strong, making it the most used 3D printer filament. The addition of carbon fiber in PLA helps in the improvement of rigidity and strength and reduces weight. Carbon fiber in the composite filament was 20%. Raise3D pro2 machine was used for making tensile specimens for testing. It had a build volume of 305 × 305 × 300 mm with features such as accurate positioning, high repeatability, and reliability. The x, y, and z-axis step sizes were only 0.78125 microns. Dog bone tensile samples were modeled in AutoCAD 2021 version 24.0. The dimensions are represented in Fig. 2. ASTM D638 Type IV was the selected standard for tensile testing.

The selected process variables and their values for PLA and PLA-CF are represented in Tables 1 and 2 respectively. Tensile strength testing experiments are conducted based on the design of experiments generated by Taguchi analysis in Minitab 2019 software. L27 orthogonal array is the available design for the 5 factors 3 levels model. Optimization of process parameters and their order of influence on ultimate tensile strength is obtained using the Taguchi method. Slicing software used for the Raise3D pro2 machine was ideaMaker 4.1.1 which helped to create the g-codes for the machine based on the experimental design. The infill design selected for printing the tensile samples is highlighted in Fig. 3. Ultimate tensile strength testing was done on Shimadzu AG-X

**Fig. 2** ASTM D638 Type IV tensile testing specimen

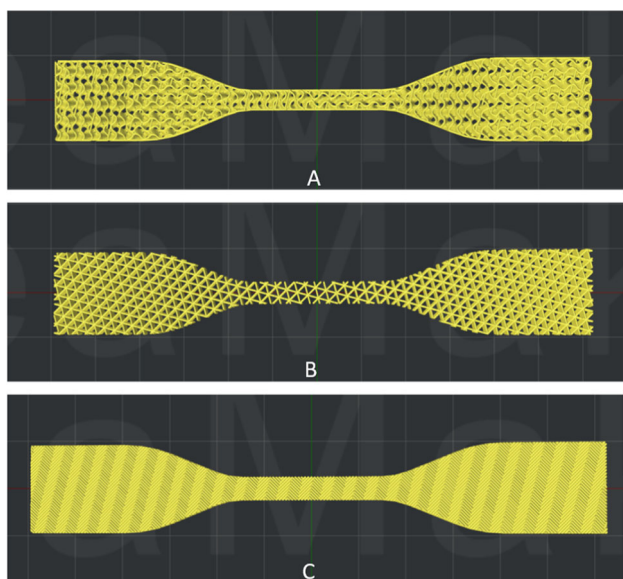
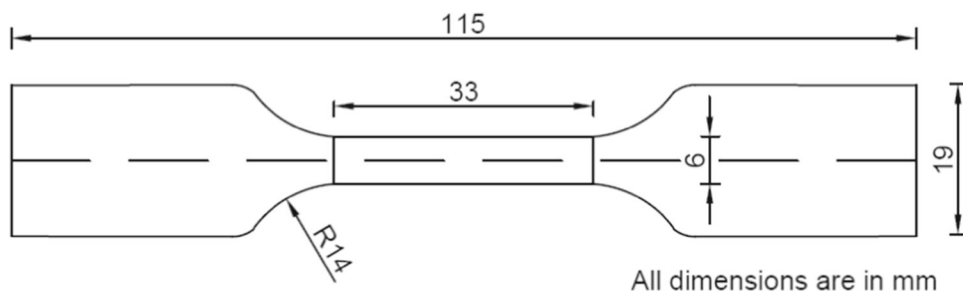


**Fig. 3** **a** Gyroid infill pattern at 30% infill volume, **b** triangle infill pattern at 60% infill volume, and **c** grid infill pattern at 90% infill volume

plus (10 kN) UTM. 3D printing and tensile testing processes are shown in Fig. 4.

Thermal annealing is the method of heating a specimen to a predetermined temperature, holding it at that temperature for a specified amount of time, then gradually cooling it down to room temperature. An annealing oven manufactured by Labline with a temperature range of 50–300 °C was utilized for the heat treatment of tensile specimens. The benefits of annealing are dependent on mainly two factors, temperature and time. Annealing conditions were chosen and their range is shown in Table 3. Annealing temperature should be selected in such a way that it is above the  $T_g$  and below the melting point of the selected material. The  $T_g$  value for PLA is around 55–60 °C, above which the molecular chain exhibit movement and displays a rubbery state [37]. Changes in crystallinity occur in amorphous and semi-crystalline materials above  $T_g$ .

Jeol JSM 6390 electron microscope was utilized to obtain the surface morphology of additively manufactured components before and after annealing. The transverse cross-sectional SEM was taken for the water jet cut surface. JSM



**Fig. 4** **a** Ultimate tensile strength testing on Shimadzu AG-X plus, **b** FFF of PLA tensile samples, and **c** FFF of PLA-CF tensile samples

**Table 3** Selected heat treatment conditions

Annealing variable	Values	Comments
Temperature	65 °C	The annealing temperature is selected between the $T_g$ and the melting point for both PLA and PLA-CF models
	95 °C	
	125 °C	
	155 °C	
Time	30 min	The time for annealing is selected from a lower duration to a higher range depending on the thickness of the samples
	60 min	
	120 min	
	240 min	

6390 had the capability of  $\times 300,000$  magnification with 3 nm resolution. A thin 10 mm glass slide was placed on sample stubs with carbon tape and gold was coated utilizing JFC 1600. This ion bombarding system coats micro specimens with gold rapidly and efficiently, improving surface visibility. The SEM tests were carried out using a 20 kV accelerating voltage and a magnification of 250 times. Bruker D8 advanced X-ray diffraction machine was employed to generate the diffraction pattern of both thermoplastics. Scanning ranges from 3 to 80° was used to obtain the intensity counts to

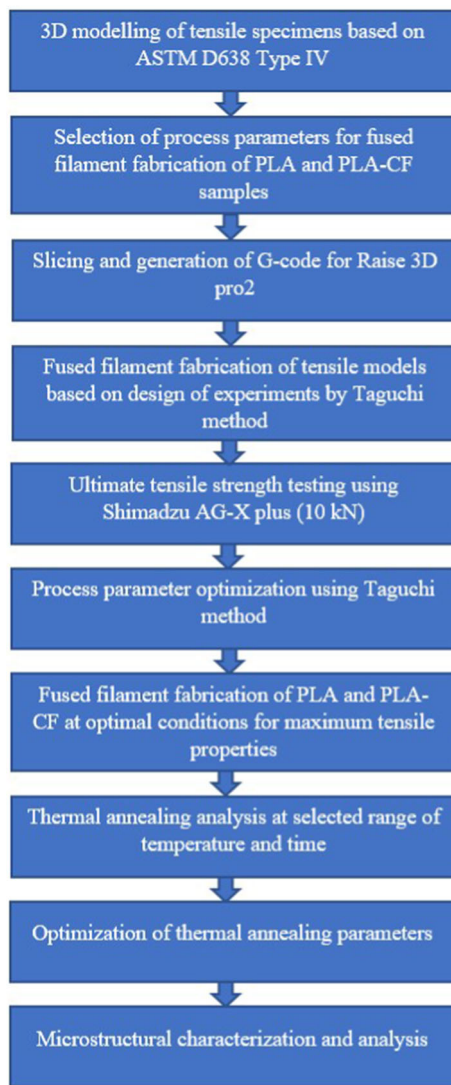


Fig. 5 Experimental Methodology

analyze the crystallinity behavior of the material. Microstructural characterization was performed to analyze the effects of annealing on the samples. An elaborated methodology of this study is presented in Fig. 5.

### 3 Results and discussion

The next sections discuss a thorough analysis of the impact of process factors and heat treatment on the ultimate tensile strength of PLA and PLA-CF.

#### 3.1 Influence of process parameters on the ultimate tensile strength of PLA and PLA-CF

The ultimate tensile strength of PLA models based on ASTM D638 Type IV at the selected process parameters is given in

Table 4. The relationship between the process variables infill percentage ( $\rho$ ), layer height ( $h$ ), extruder temperature ( $T$ ), print velocity ( $V$ ), and response parameter ultimate tensile strength ( $\sigma_u$ ) is shown in Eqs. 1, 2, and 3.

For triangle infill patterns,

$$\sigma_{u, tr} = 15.1172 + 0.0875\rho - 11.2667h + 0.0486T - 0.0789V \quad (1)$$

For grid infill patterns,

$$\sigma_{u, gr} = 14.7817 + 0.0875\rho - 11.2667h + 0.0486T - 0.0789V \quad (2)$$

For gyroid infill patterns,

$$\sigma_{u, gy} = 16.2061 + 0.0875\rho - 11.2667h + 0.0486T - 0.0789V \quad (3)$$

The  $R^2$  value of the regression equations for PLA is obtained as 85.57%. The ultimate tensile strength of 20% PLA-CF models based on ASTM D638 Type IV at the selected process parameters is shown in Table 5. The relationship between the selected process parameters and the response variable ultimate tensile strength for PLA-CF is shown in Eqs. 4, 5, and 6.

For triangle infill patterns,

$$\sigma_{u, tr} = 25.6311 + 0.0736\rho - 9.2726h + 0.0288T - 0.0424V \quad (4)$$

For grid infill patterns,

$$\sigma_{u, gr} = 25.9419 + 0.0736\rho - 9.2726h + 0.0288T - 0.0424V \quad (5)$$

For gyroid infill patterns,

$$\sigma_{u, gy} = 26.5057 + 0.0736\rho - 9.2726h + 0.0288T - 0.0424V \quad (6)$$

The  $R^2$  value of the regression equations for PLA-CF is obtained as 91.81%. The main effects plot for means and SN ratios of PLA and PLA-CF with respect to the process parameters are shown in Figs. 6 and 7 respectively. The analysis of variance and response table for SN ratios of PLA are shown in Tables 6 and 7 respectively. Tables 8 and 9 show the analysis of variance and response table for SN ratios of PLA-CF.

Infill volume, printing speed, pattern, layer height, and extruder temperature have the most influence on the ultimate tensile strength of PLA. The ranking order of the

**Table 4** Ultimate tensile strength of PLA

Infill percentage (%)	Infill pattern	Layer height (mm)	Extruder temperature (°C)	Print speed (mm/s)	Ultimate tensile strength (MPa)
30	Triangle	0.1	200	30	24.39
30	Triangle	0.1	200	45	21.89
30	Triangle	0.1	200	60	21.68
30	Grid	0.15	210	30	25.12
30	Grid	0.15	210	45	21.23
30	Grid	0.15	210	60	20.87
30	Gyroid	0.2	220	30	24.86
30	Gyroid	0.2	220	45	23.89
30	Gyroid	0.2	220	60	22.01
60	Triangle	0.15	220	30	27.09
60	Triangle	0.15	220	45	24.78
60	Triangle	0.15	220	60	25.12
60	Grid	0.2	200	30	25.16
60	Grid	0.2	200	45	23.67
60	Grid	0.2	200	60	23.25
60	Gyroid	0.1	210	30	26.47
60	Gyroid	0.1	210	45	27.45
60	Gyroid	0.1	210	60	28.47
90	Triangle	0.2	210	30	29.14
90	Triangle	0.2	210	45	26.76
90	Triangle	0.2	210	60	27.09
90	Grid	0.1	220	30	29.17
90	Grid	0.1	220	45	30.78
90	Grid	0.1	220	60	25.67
90	Gyroid	0.15	200	30	30.23
90	Gyroid	0.15	200	45	28.18
90	Gyroid	0.15	200	60	26.18

impact of process variables on the tensile strength of PLA-CF is infill volume, printing speed, layer height, pattern, and extruder temperature. As the material percentage increases, the mechanical strength of printed components increases significantly. The volume of infill for each specimen is the most crucial parameter influencing ultimate tensile strength. Layer height and print speed are inversely proportional to ultimate tensile strength. As the thickness of each layer rises, the possibility of voids creation becomes dominant and thereby reduces tensile strength. Low printing velocity helps in the successful completion of the printing of complex geometries. As printing speed increases, vibrations occur and interlayer adhesion weakens affecting its mechanical strength. The gyroid pattern produced maximum strength for both materials. These patterns were able to produce higher strength in lower infill density specimens too. The curvy pattern is thus a possible solution for high strength-to-weight ratio

applications. Nozzle temperature had the least influence on the ultimate tensile strength. From the plots, it is clear that the increase in extruder temperature slightly improved the strength which might be due to the proper melting of thermoplastics. The highest tensile strength of 31.11 MPa was achieved for PLA tensile model at the optimized process parameters printing conditions. PLA-CF showed an ultimate tensile strength of 37.27 MPa at the optimized printing parameters. PLA-CF showcased higher strength than normal PLA tensile specimens.

### 3.2 Impact of heat treatment parameters on the ultimate tensile strength of PLA and PLA-CF

A further study was made to understand the influences of annealing on the ultimate tensile strength of PLA and

**Table 5** Ultimate tensile strength of PLA-CF [38]

Infill percentage (%)	Infill pattern	Layer height (mm)	Extruder temperature (°C)	Print velocity (mm/s)	Ultimate tensile strength (MPa)
30	Grid	0.15	220	30	30.8513
30	Grid	0.15	220	45	31.2447
30	Grid	0.15	220	60	31.0091
30	Gyroid	0.2	230	30	31.7326
30	Gyroid	0.2	230	45	31.6469
30	Gyroid	0.2	230	60	30.8304
30	Triangle	0.1	210	30	31.7155
30	Triangle	0.1	210	45	30.3744
30	Triangle	0.1	210	60	30.5494
60	Grid	0.1	230	30	35.0897
60	Grid	0.1	230	45	33.6886
60	Grid	0.1	230	60	34.6519
60	Triangle	0.2	220	30	33.1438
60	Triangle	0.2	220	45	33.3607
60	Triangle	0.2	220	60	32.0511
60	Gyroid	0.15	210	30	34.6885
60	Gyroid	0.15	210	45	33.6053
60	Gyroid	0.15	210	60	34.0653
90	Gyroid	0.1	220	30	37.2672
90	Gyroid	0.1	220	45	35.8946
90	Gyroid	0.1	220	60	35.9219
90	Triangle	0.15	230	30	36.7693
90	Triangle	0.15	230	45	35.8083
90	Triangle	0.15	230	60	34.0086
90	Grid	0.2	210	30	36.4649
90	Grid	0.2	210	45	34.3954
90	Grid	0.2	210	60	33.1821

PLA-CF. The importance of thermal annealing for strength enhancement had been researched in the past [39, 40]. This work demonstrates detailed analysis of thermal annealing conditions to optimize their level to maximize the tensile strength. The significance of thermal annealing in FFF is that the process itself is based on the material extrusion at high temperatures and rapid cooling which will eventually create stress and reduce crystallinity within the samples. Ultimate tensile strength values of PLA and PLA-CF after the heat treatment process at temperatures of 65, 95, 125, and 155 °C at different durations of 30, 60, 120, and 240 min are shown in Table 10.

The annealing temperatures were chosen with the materials' glass transition and melting temperatures in reference. The  $T_g$  of PLA lies around 60 °C. Annealing above glass transition results in re-arrangement of molecular chains and improvement of crystallinity. Highest tensile strength of

38.27 MPa was attained for PLA dog bone samples after annealing at 95 °C for 1 h duration. Highest tensile strength of 42.49 MPa was obtained for PLA-CF tensile models after annealing at 95 °C for 2 h. A large duration time did not significantly improve the mechanical strength of both specimens. Annealing temperatures above cold crystallization showed no improvement in tensile strength. The cold crystallization point of PLA lies around 110–115 °C. Degradation of polymer chains at elevated temperatures for a longer duration resulted in lower mechanical strength of thermoplastics. The impact of annealing on PLA tensile models exhibited an improvement of 23.02% whereas PLA-CF displayed an increase of 14.01% for the ultimate tensile strength values. Annealing effects were studied on the fully solid tensile specimen and the results are represented in Fig. 8.

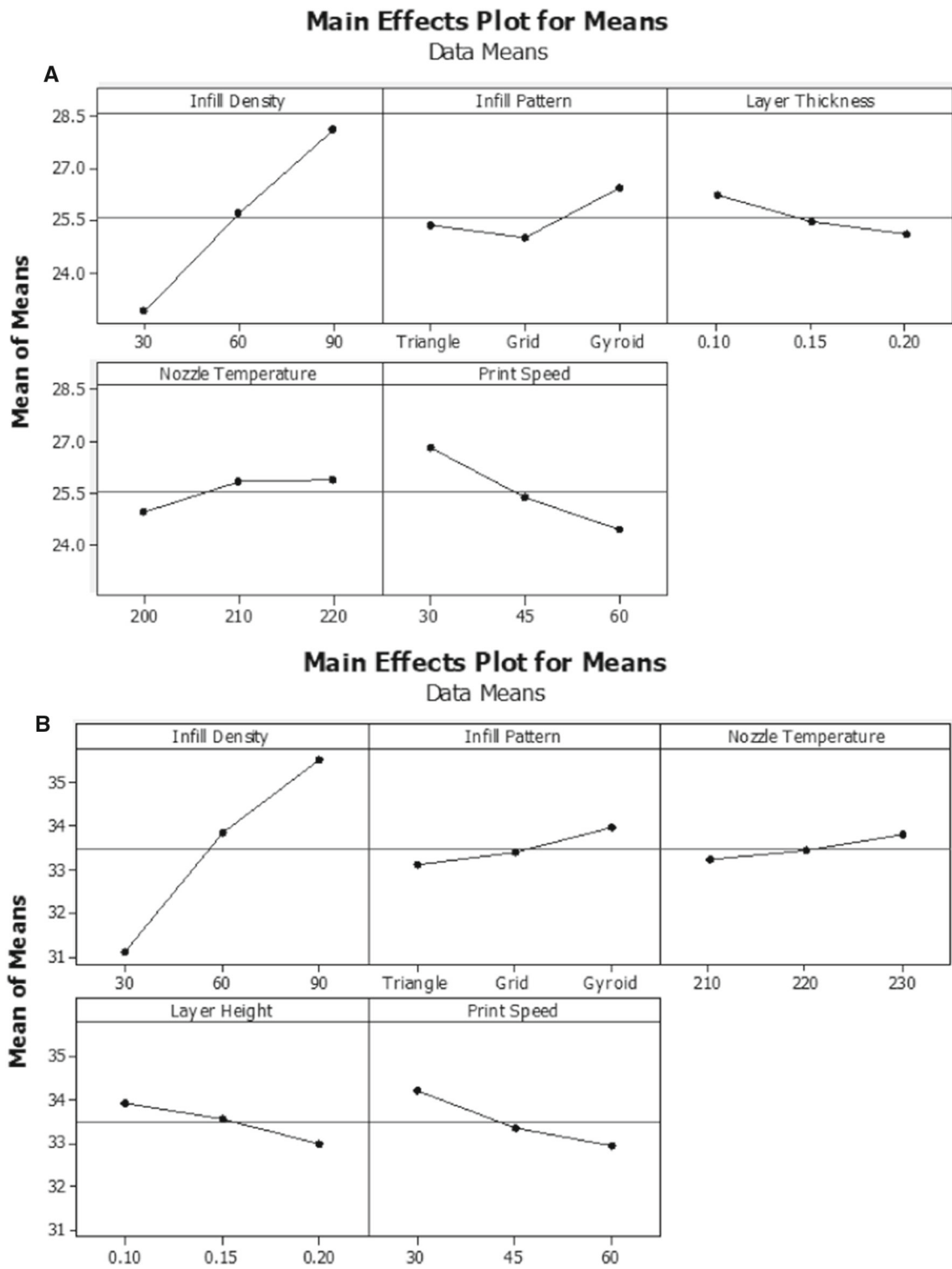
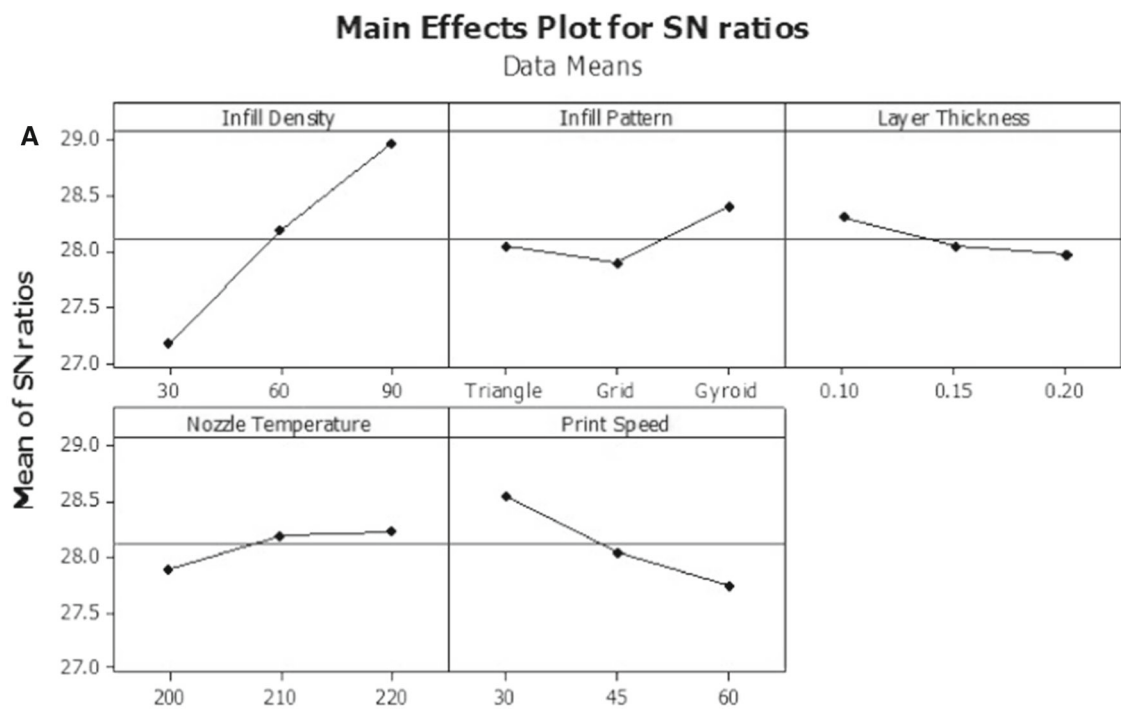
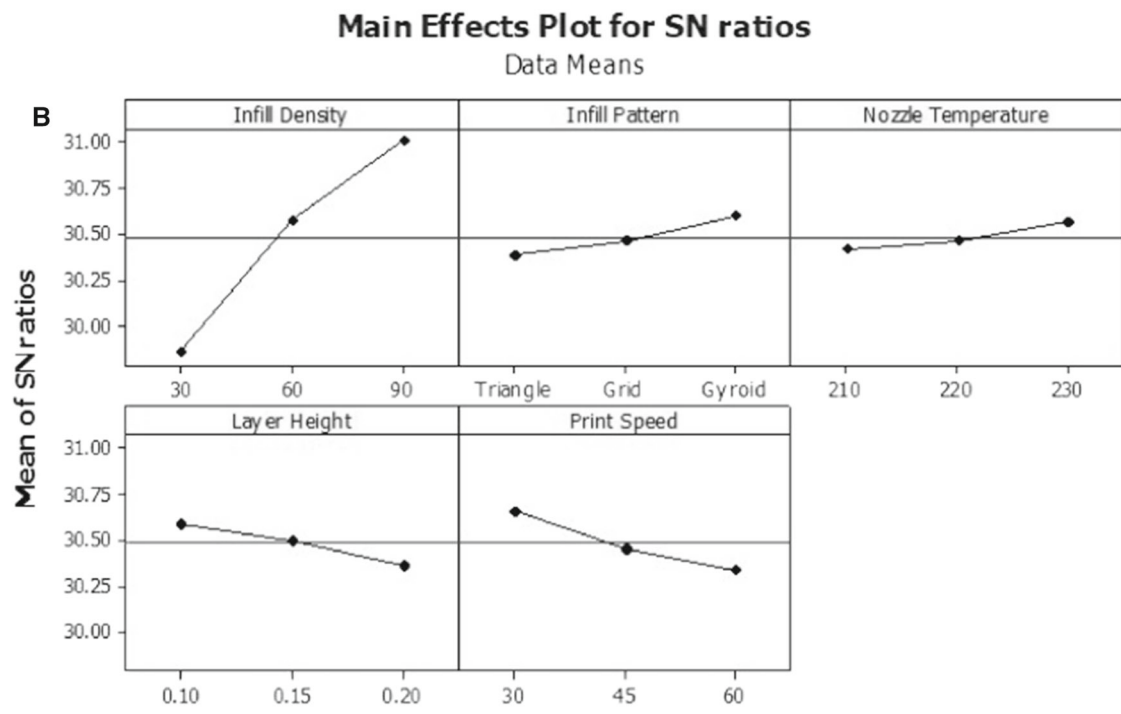


Fig. 6 Main effects plot for means of a PLA and, b PLA-CF





Signal-to-noise: Larger is better



Signal-to-noise: Larger is better

Fig. 7 Main effects plot for SN ratios of a PLA and, b PLA-CF

**Table 6** Analysis of variance for PLA samples

Source	DF	Seq SS	Adj SS	Adj MS	F	P
Infill density	2	14.6419	14.6419	7.3210	39.97	0.000
Infill pattern	2	1.2493	1.2493	0.6246	3.41	0.051
Layer thickness	2	0.6128	0.6128	0.3064	1.67	0.219
Nozzle temperature	2	0.6158	0.6158	0.3079	1.68	0.217
Print velocity	2	3.0992	3.0992	1.5496	8.46	0.003
Residual error	16	2.9305	2.9305	0.1832		
Total	26	23.1495				

**Table 7** Response table for SN ratios of PLA samples

Level	Infill density	Infill pattern	Layer height	Nozzle temperature	Print velocity
1	27.17	28.03	28.32	27.90	28.55
2	28.19	27.89	28.05	28.19	28.04
3	28.97	28.40	27.96	28.24	27.73
Delta	1.80	0.51	0.35	0.34	0.82
Rank	1	3	4	5	2

**Table 8** Analysis of variance for PLA-CF samples

Source	DF	Seq SS	Adj SS	Adj MS	F	P
Infill density	2	6.0715	6.0715	3.03577	104.53	0.000
Infill pattern	2	0.2369	0.2369	0.11843	4.08	0.037
Nozzle temperature	2	0.1063	0.1063	0.05317	1.83	0.192
Layer thickness	2	0.2432	0.2432	0.12161	4.19	0.034
Print velocity	2	0.4857	0.4857	0.24283	8.36	0.003
Residual error	16	0.4647	0.4647	0.02904		
Total	26	7.6083				

### 3.3 Influence of annealing on crystallinity and microstructures of PLA and PLA-CF

XRD tests were performed on annealed and non-annealed PLA and PLA-CF to study the impacts of heat treatment on the specimens. Figure 8 demonstrates the diffraction patterns obtained for both thermoplastics with the scanning ranges from 3 to 80°. Both PLA and PLA-CF behaved as an amorphous materials without heat treatment. Crystallinity peaks were found on thermally annealed 3D printed samples. Maximum intensity peak was observed at a  $2\theta$  of 16.772°. PLA

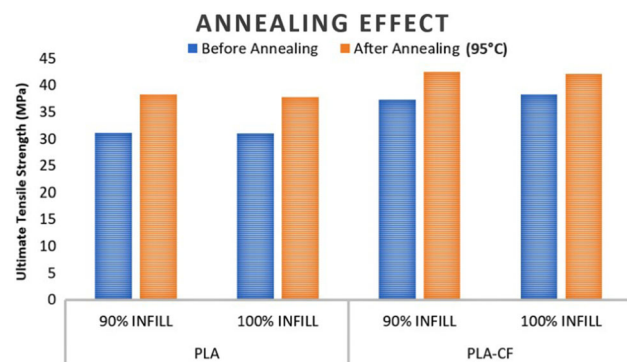
displayed a crystallinity percentage of only 3.91% whereas annealing of PLA at 95 °C for 1 h duration increased the crystallinity index to 28.7%. More crystalline planes were formed after the optimal heat treatment. The crystallinity index of PLA-CF increased from 5.93 to 30.86% after the heat treatment at 95 °C for 2 h duration. The non-annealed samples had a large amorphous region without crystalline peaks. This could be a reason for the strength enhancement of thermoplastic PLA and PLA-CF at optimum annealing conditions. The XRD plots are shown in Fig. 9.

**Table 9** Response table for SN ratios of PLA-CF samples

Level	Infill density	Infill pattern	Nozzle temperature	Layer thickness	Print velocity
1	29.86	30.38	30.42	30.58	30.66
2	30.58	30.46	30.46	30.50	30.45
3	31.00	30.60	30.57	30.35	30.34
Delta	1.15	0.23	0.15	0.23	0.32
Rank	1	4	5	3	2

**Table 10** Mechanical strength of PLA and PLA-CF after thermal annealing

Annealing temperature (°C)	Annealing time (min)	Tensile strength of PLA (MPa)	Tensile strength of PLA-CF (MPa)
65	30	31.57	36.45
65	60	29.92	37.82
65	120	30.78	36.34
65	240	30.45	36.89
95	30	33.89	37.59
95	60	38.27	40.23
95	120	36.71	42.49
95	240	31.69	38.28
125	30	34.57	37.44
125	60	34.13	38.54
125	120	33.45	37.61
125	240	30.12	37.07
155	30	31.98	36.67
155	60	29.67	35.23
155	120	27.33	35.88
155	240	27.56	34.73

**Fig. 8** Comparative plots of ultimate tensile strength of PLA and PLA-CF

SEM imaging was also conducted on these samples to study the surface morphology. Both transverse and longitudinal sections were examined and the micrographs are given in Figs. 10 and 11 respectively. Micrographs showed improvement in the merging of layers and this interlayer diffusion could be a reason for the strength improvement after the annealing process. Although the outer surface exposed to direct temperature had flaky or blistered nature, the interlayer and raster bonding was found to be strong. SEM imaging with 250 times magnification was utilized for studying the surface patterns. The increase in volume on account of the

larger density of crystalline area could be observed from the micro-analysis. These characterization techniques strengthened the authenticity of the experimental data on the ultimate tensile strength of fused filament fabricated thermoplastics.

## 4 Conclusions

The impact of parametric analysis and thermal annealing on the ultimate tensile strength and microstructure of PLA and PLA-CF were studied. Proper choice of process parameters aids in improving the tensile properties of FFF components. Process parameters were ranked according to their impact on the response variable in the order of infill volume, print velocity, pattern, layer height, and extruder temperature. The highest tensile strength was obtained for maximum infill percentage where the amount of material significantly influences strength values. The gyroid infill pattern showed maximum tensile strength for both PLA and PLA-CF as the wavy pattern helps in building strong interlayer bonds. PLA and PLA-CF dog bone specimens produced 31.11 and 37.27 MPa tensile strength respectively at the optimized processing conditions. Annealing of PLA samples at 95 °C for 1 h duration revealed a maximum ultimate tensile strength of 38.27 MPa, yielding a 23.02% improvement in strength compared to the normal PLA. Annealing of PLA-CF samples at 95 °C for 2 h duration showed a maximum ultimate tensile strength of 42.49 MPa, yielding a 14.01% improvement in strength compared to the normal PLA-CF. Ultimate tensile strength showed improvement at the selected annealing temperature between  $T_g$  and cold crystallization temperature. X-ray diffraction results proved the growth in the crystallinity percentage after the heat treatment process and SEM micrographs showed good diffusion and interlayer bonding after thermal annealing post-processing.

Process parameter optimization and thermal annealing heat treatment process could definitely enhance the mechanical strength of fused filament fabricated thermoplastics. This study involved the detailed analysis of annealing conditions on the ultimate tensile strength of PLA as well as composite PLA. The selection of optimized parameters and annealing conditions strengthened the 3D printed models. The distortion effects on the specimen due to thermal annealing can be considered a future scope of this study. The applications which demand a high strength-to-weight ratio can obviously adapt these processing methods. The thermal stability of material extrusion-based additive manufacturing might be enhanced by implementing a thermal annealing process. The growth of 3D printing and its applications can be advanced by employing appropriate heat treatment post-processing methodology.

## X-RAY DIFFRACTION PATTERNS

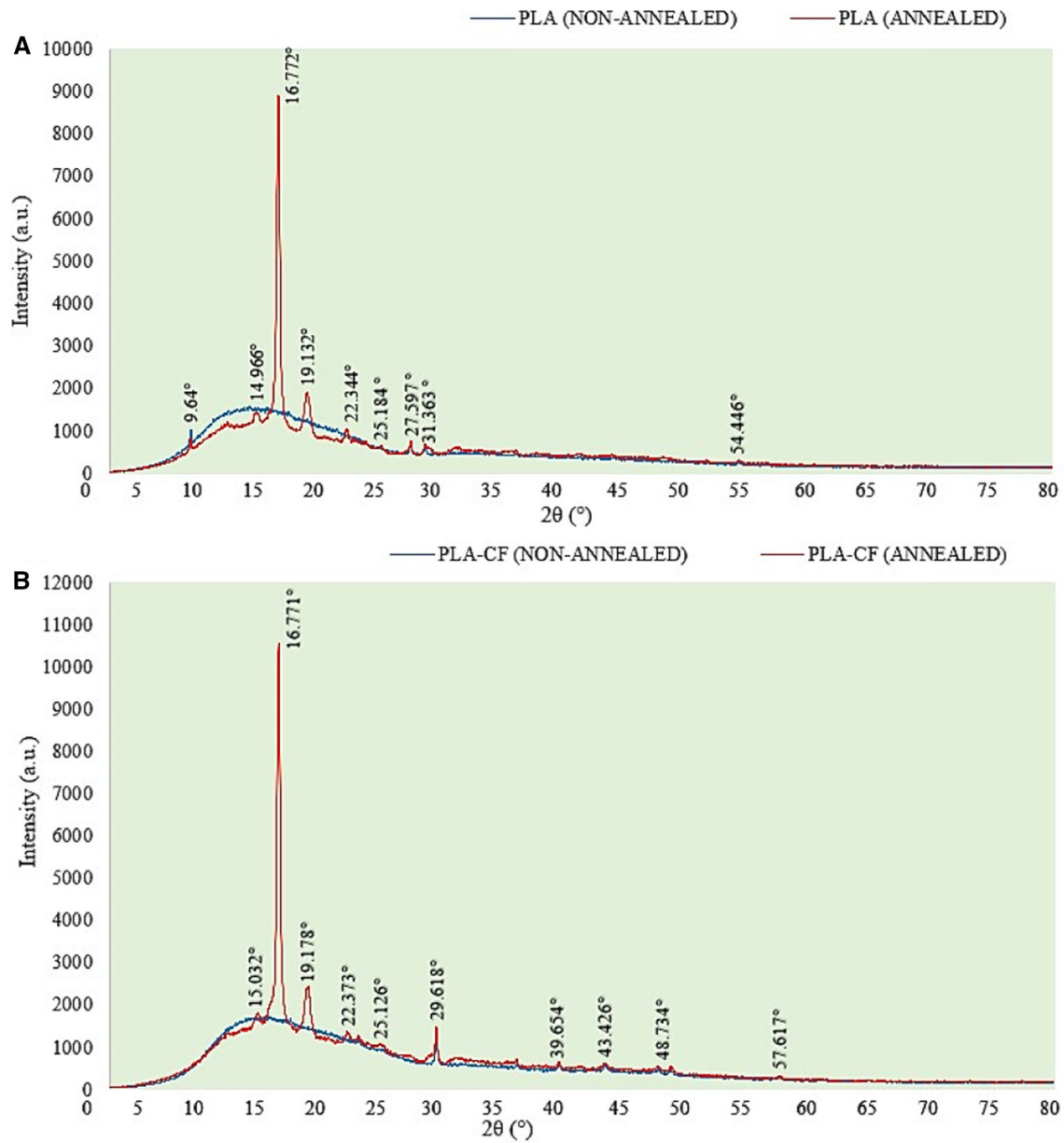


**Fig. 9** XRD results of fused filament fabricated **a** PLA, and **b** PLA-CF

pt

**Fig. 10** SEM micrographs of the transverse cross-section of **a** Non-annealed PLA, **b** PLA annealed at 95 °C for 1 h, **c** Non-annealed PLA-CF, and **d** PLA-CF annealed at 95 °C for 2 h

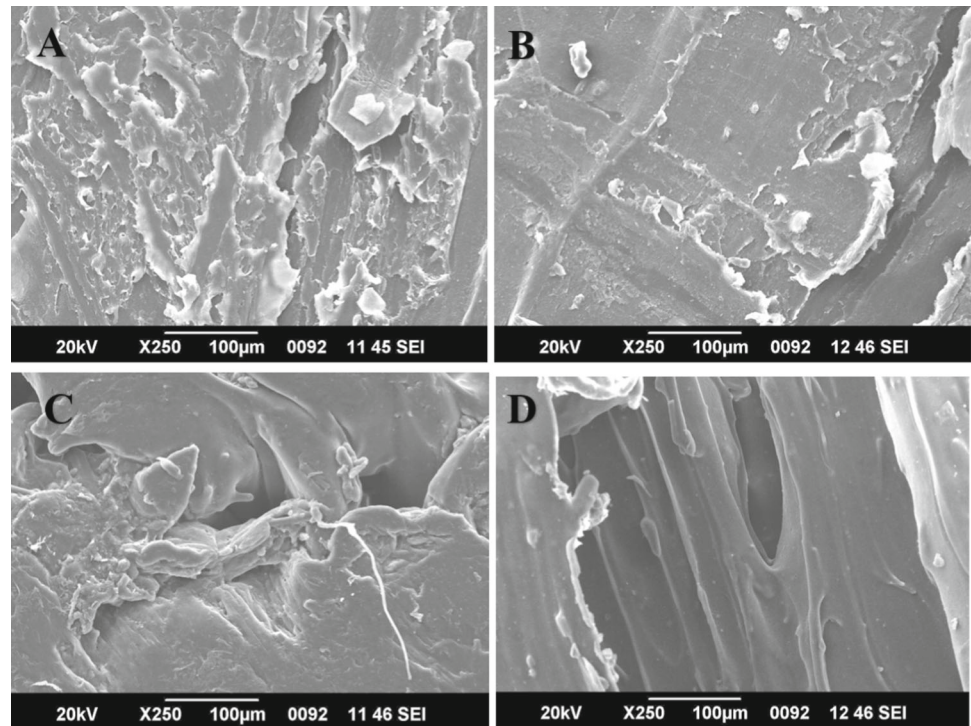
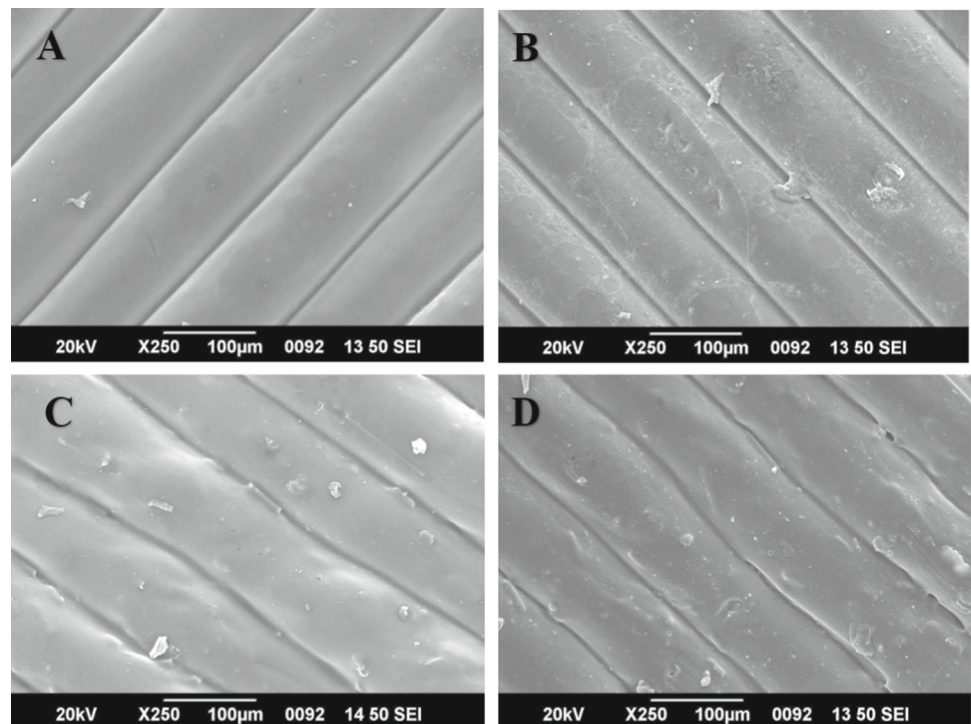


**Fig. 11** SEM micrographs of a longitudinal cross-section of **a** Non-annealed PLA, **b** PLA annealed at 95 °C for 1 h, **c** Non-annealed PLA-CF, and **d** PLA-CF annealed at 95 °C for 2 h



**Acknowledgements** The authors extend their appreciation to the Principal and HOD of Mechanical Engineering, GCE Kannur for the research facilities given. The authors acknowledge TEQIP Four Funds, GCE Kannur for the financial aid.

**Funding** The authors state that they do not have any known competing financial interests or personal connections that may seem to have influenced the work disclosed in this study.

## References

- Mitchell, A., Lafont, U., Holyńska, M., Semprimoschnig, C.: Additive manufacturing—A review of 4D printing and future applications. *Addit. Manuf.* **24**, 606–626 (2018). <https://doi.org/10.1016/j.addma.2018.10.038>
- Ghilan, A., Chiriac, A.P., Nita, L.E., Rusu, A.G., Neamtu, I., Chiriac, V.M.: Trends in 3D printing processes for biomedical field: opportunities and challenges. *J. Polym. Environ.* **28**(5), 1345–1367 (2020). <https://doi.org/10.1007/s10924-020-01722-X>
- Stansbury, J.W., Idacavage, M.J.: 3D printing with polymers: challenges among expanding options and opportunities. *Dent. Mater. J.* **32**(1), 54–64 (2016). <https://doi.org/10.1016/j.dental.2015.09.018>
- Prashar, G., Vasudev, H., Bhuddhi, D.: Additive manufacturing: expanding 3D printing horizon in industry 4.0. *Int. J. Interact. Des. Manuf.* (2022). <https://doi.org/10.1007/s12008-022-00956-4>
- Yadav, A., Rohru, P., Babbar, A., Kumar, R., Ranjan, N., Chohan, J.S., Kumar, R., Gupta, M.: Fused filament fabrication: a state-of-the-art review of the technology, materials, properties and defects. *Int. J. Interact. Des. Manuf.* (2022). <https://doi.org/10.1007/s12008-022-01026-5>
- Guo, N., Leu, M.C.: Additive manufacturing: technology, applications and research needs. *Front. Mech. Eng.* **8**(3), 215–243 (2013). <https://doi.org/10.1007/s11465-013-0248-8>
- Backes, E.H., Pires, L.D.N., Beatrice, C.A.G., Costa, L.C., Passador, F.R., Pessan, L.A.: Fabrication of biocompatible composites of poly (lactic acid)/hydroxyapatite envisioning medical applications. *Polym. Eng. Sci.* **60**(3), 636–644 (2020). <https://doi.org/10.1002/PEN.25322>
- Lee, J.Y., An, J., Chua, C.K.: Fundamentals and applications of 3D printing for novel materials. *Appl. Mater. Today* **7**, 120–133 (2017). <https://doi.org/10.1016/j.apmt.2017.02.004>
- Sathies, T., Senthil, P., Anoop, M.S.: A review on advancements in applications of fused deposition modelling process. *Rapid Prototyp. J.* **26**(4), 669–687 (2020). <https://doi.org/10.1108/RPJ-08-2018-0199>
- Nayak, C., Singh, A., Chaudhary, H., Tripathi, A.: A novel approach for customized prosthetic socket design. *Biomed. Eng.* **28**(03), 1650022 (2016). <https://doi.org/10.4015/S1016237216500228>
- Zein, I., Hutmacher, D.W., Teoh, S.H., Tan, K.C.: Poly (ε-caprolactone) scaffolds designed and fabricated by fused deposition modeling. *Biomaterials* **23**(4), 1169–1185 (2002). [https://doi.org/10.1016/S0142-9612\(01\)00232-0](https://doi.org/10.1016/S0142-9612(01)00232-0)
- Singh, S., Ramakrishna, S.: Biomedical applications of additive manufacturing: present and future. *Curr. Opin. Biomed. Eng.* **2**, 105–115 (2017). <https://doi.org/10.1016/j.cobme.2017.05.006>
- Bhat, A., Budholiya, S., Raj, S.A., Sultan, M.T.H., Hui, D., Shah, A.U.M., Safri, S.N.A.: Review on nanocomposites based on aerospace applications. *Nanotechnol. Rev.* **10**(1), 237–253 (2021). <https://doi.org/10.1515/ntrev-2021-0018>
- Jeong, H.Y., An, S.C., Lim, Y., Jeong, M.J., Kim, N., Jun, Y.C.: 3D and 4D printing of multistable structures. *Appl. Sci.* **10**(20), 7254 (2020). <https://doi.org/10.3390/app10207254>
- Masood, S.H., Song, W.Q.: Development of new metal/polymer materials for rapid tooling using fused deposition modelling. *Mater. Des.* **25**(7), 587–594 (2004). <https://doi.org/10.1016/j.matdes.2004.02.009>
- Donate, R., Monzón, M., Alemán-Domínguez, M.E.: Additive manufacturing of PLA-based scaffolds intended for bone regeneration and strategies to improve their biological properties. *e-Polym.* **20**(1), 571–599 (2020). <https://doi.org/10.1515/epoly-2020-0046>
- Liao, Y., Liu, C., Coppola, B., Barra, G., Di Maio, L., Incarnato, L., Lafdi, K.: Effect of porosity and crystallinity on 3D printed PLA properties. *Polymers* **11**(9), 1487 (2019). <https://doi.org/10.1515/epoly-2020-0046>
- Sunny, S., Chen, H., Malik, A., Lu, H.: Influence of residual stress and fluid–structure interaction on the impact behavior of fused filament fabrication components. *Addit. Manuf.* **37**, 101662 (2021). <https://doi.org/10.1016/j.addma.2020.101662>
- de Pastre, M.A., Quinsat, Y., Lartigue, C.: Effects of additive manufacturing processes on part defects and properties: a classification review. *Int. J. Interact. Des. Manuf.* (2022). <https://doi.org/10.1007/s12008-022-00839-8>
- Taufik, M., Jain, P.K.: Thermally assisted finishing of fused deposition modelling build part using a novel CNC tool. *J. Manuf. Process.* **59**, 266–278 (2020). <https://doi.org/10.1016/j.jmapro.2020.09.060>
- Valerga, A.P., Batista, M., Fernandez-Vidal, S.R., Gamez, A.J.: Impact of chemical post-processing in fused deposition modelling (FDM) on polylactic acid (PLA) surface quality and structure. *Polymers* **11**(3), 566 (2019). <https://doi.org/10.3390/polym11030566>
- Nguyen, T.K., Lee, B.K.: Post-processing of FDM parts to improve surface and thermal properties. *Rapid Prototyp. J.* **24**(7), 1091–1100 (2018). <https://doi.org/10.1108/RPJ-12-2016-0207>
- Karakurt, I., Lin, L.: 3D printing technologies: techniques, materials, and post-processing. *Curr. Opin. Chem. Eng.* **28**, 134–143 (2020). <https://doi.org/10.1016/j.coche.2020.04.001>
- Mu, M., Ou, C.Y., Wang, J., Liu, Y.: Surface modification of prototypes in fused filament fabrication using chemical vapour smoothing. *Addit. Manuf.* **31**, 100972 (2020). <https://doi.org/10.1016/j.addma.2019.100972>
- Singh, S., Rajeshkannan, A., Feroz, S., Jeevanantham, A.K.: Effect of normalizing on the tensile strength, shrinkage and surface roughness of PLA plastic. *Mater. Today Proc.* **24**, 1174–1182 (2020). <https://doi.org/10.1016/j.matpr.2020.04.431>
- Zaldivar, R.J., Witkin, D.B., McLouth, T., Patel, D.N., Schmitt, K., Nokes, J.P.: Influence of processing and orientation print effects on the mechanical and thermal behavior of 3D-Printed ULTEM@ 9085 Material. *Addit. Manuf.* **13**, 71–80 (2017). <https://doi.org/10.1016/j.addma.2016.11.007>
- Pérez, M., Medina-Sánchez, G., García-Collado, A., Gupta, M., Carou, D.: Surface quality enhancement of fused deposition modeling (FDM) printed samples based on the selection of critical printing parameters. *Materials* **11**(8), 1382 (2018). <https://doi.org/10.3390/ma11081382>
- Nath, P., Olson, J.D., Mahadevan, S., Lee, Y.T.T.: Optimization of fused filament fabrication process parameters under uncertainty to maximize part geometry accuracy. *Addit. Manuf.* **35**, 101331 (2020). <https://doi.org/10.1016/j.addma.2020.101331>
- Li, H., Wang, T., Sun, J., Yu, Z.: The effect of process parameters in fused deposition modelling on bonding degree and mechanical properties. *Rapid Prototyp. J.* **24**(1), 80–92 (2018). <https://doi.org/10.1108/RPJ-06-2016-0090>
- Wach, R.A., Wolszczak, P., Adamus-Włodarczyk, A.: Enhancement of mechanical properties of FDM-PLA parts via thermal annealing. *Macromol. Mater. Eng.* **303**(9), 1800169 (2018). <https://doi.org/10.1002/mame.201800169>
- Dong, J., Mei, C., Han, J., Lee, S., Wu, Q.: 3D printed poly (lactic acid) composites with grafted cellulose nanofibers: effect of nanofiber and post-fabrication annealing treatment on composite

- flexural properties. *Addit. Manuf.* **28**, 621–628 (2019). <https://doi.org/10.1016/j.addma.2019.06.004>
32. Ivey, M., Melenka, G.W., Carey, J.P., Ayranci, C.: Characterizing short-fiber-reinforced composites produced using additive manufacturing. *Adv. Manuf. Polym. Compos. Sci.* **3**(3), 81–91 (2017). <https://doi.org/10.1080/20550340.2017.1341125>
  33. Bhandari, S., Lopez-Anido, R.A., Gardner, D.J.: Enhancing the interlayer tensile strength of 3D printed short carbon fiber reinforced PETG and PLA composites via annealing. *Addit. Manuf.* **30**, 100922 (2019). <https://doi.org/10.1016/j.addma.2019.100922>
  34. Rane, R., Kulkarni, A., Prajapati, H., Taylor, R., Jain, A., Chen, V.: Post-process effects of isothermal annealing and initially applied static uniaxial loading on the ultimate tensile strength of fused filament fabrication parts. *Materials* **13**(2), 352 (2020). <https://doi.org/10.3390/ma13020352>
  35. Wootthikanokkhan, J., Cheachun, T., Sombatsompop, N., Thumsorn, S., Kaabuaathong, N., Wongta, N., Wong-On, J., Na Ayuthaya, S.I., Kositchaiyong, A.: Crystallization and thermomechanical properties of PLA composites: effects of additive types and heat treatment. *J. Appl. Polym. Sci.* **129**(1), 215–223 (2013). <https://doi.org/10.1002/app.38715>
  36. El Magri, A., El Mabrouk, K., Vaudreuil, S., Chibane, H., Touhami, M.E.: Optimization of printing parameters for improvement of mechanical and thermal performances of 3D printed poly (ether ether ketone) parts. *J. Appl. Polym. Sci.* **137**(37), 49087 (2020). <https://doi.org/10.1002/app.49087>
  37. Akhouni, B., Nabipour, M., Hajami, F., Shakoory, D.: An experimental study of nozzle temperature and heat treatment (annealing) effects on mechanical properties of high-temperature polylactic acid in fused deposition modeling. *Polym. Eng. Sci.* **60**(5), 979–987 (2020). <https://doi.org/10.1002/pen.25353>
  38. Arjun, P., Bidhun, V.K., Lenin, U.K., Amritha, V.P., Pazhamannil, R.V., Govindan, P.: Effects of process parameters and annealing on the tensile strength of 3D printed carbon fiber reinforced polylactic acid. *Mater. Today Proc.* **62**(14), 7389–7394 (2022). <https://doi.org/10.1016/j.matpr.2022.02.142>
  39. Prajapati, H., Chalise, D., Ravoori, D., Taylor, R.M., Jain, A.: Improvement in build-direction thermal conductivity in extrusion-based polymer additive manufacturing through thermal annealing. *Addit. Manuf.* **26**, 242–249 (2019). <https://doi.org/10.1016/j.addma.2019.01.004>
  40. Dunn, R.M., Hart, K.R., Wetzel, E.D.: Improving fracture strength of fused filament fabrication parts via thermal annealing in a printed support shell. *Prog. Addit. Manuf.* **4**(3), 233–243 (2019). <https://doi.org/10.1007/s40964-019-00081>

**Publisher's Note** Springer Nature remains neutral with regard to jurisdictional claims in published maps and institutional affiliations.

Springer Nature or its licensor (e.g. a society or other partner) holds exclusive rights to this article under a publishing agreement with the author(s) or other rightsholder(s); author self-archiving of the accepted manuscript version of this article is solely governed by the terms of such publishing agreement and applicable law.